European Journal of Medicinal Chemistry 44 (2009) 4218–4226

Contents lists available at ScienceDirect

European Journal of Medicinal Chemistry

journal homepage: http://www.elsevier.com/locate/ejmech

Original article

New azoles with potent antifungal activity: Design, synthesis and molecular docking

Xiaoying Che [a], Chunquan Sheng [a,**], Wenya Wang [a], Yongbing Cao [a], Yulan Xu [a], Haitao Ji [b], Guoqiang Dong [a], Zhenyuan Miao [a], Jianzhong Yao [a], Wannian Zhang [a,*]

[a] School of Pharmacy, Second Military Medical University, 325 Guohe Road, Shanghai 200433, People's Republic of China
[b] Department of Chemistry, Department of Biochemistry, Molecular Biology and Cell Biology and Center for Drug Discovery and Chemical Biology, Northwestern University, Evanston, IL 60208-3113, USA

ARTICLE INFO

Article history:
Received 22 April 2009
Received in revised form 17 May 2009
Accepted 19 May 2009
Available online 24 May 2009

Keywords:
Azole
Rational design
Molecular docking
Antifungal activity

ABSTRACT

In response to the urgent need for novel antifungal agents with improved activity and broader spectrum, computer modeling was used to rational design novel antifungal azoles. On the basis of the active site of lanosterol 14α-demethylase from *Candida albicans* (CACYP51), a series of new azoles with substituted-phenoxypropyl piperazine side chains were rational designed and synthesized. *In vitro* antifungal activity assay indicates that the new azoles show good activity against most of the tested pathogenic fungi. Interestingly, the designed compounds are also active against an azole-resistant clinical strain. Compared to fluconazole and itraconazole, several compounds (such as **12i**, **12j** and **12n**) show higher antifungal activity and broader spectrum, which are promising leads for the development of novel antifungal agents.

1. Introduction

During the past two decades, fungal infection has become an important complication and a major cause of morbidity and mortality in immunocompromised individuals such as patients undergoing anticancer chemotherapy or organ transplants and patients with AIDS [1]. Clinically, candidosis, aspergillosis and cryptococcosis are the three major fungal infections in immunocompromised individuals [2,3]. The common antifungal agents currently used in clinic are azoles (such as fluconazole, ketoconazole and itraconazole) [4], polyenes (such as amphotericin B [5] and nystatin [6]), echinocandins (such as caspofungin and micafungin) [7] and allylamines (such as naftifine and terbinafine) [8]. Among those, azoles are widely used in antifungal chemotherapy. Fluconazole is preferred as first-line antifungal therapy with good antifungal activity and relatively low toxicity [9]. However, fluconazole is not effective against invasive aspergillosis and has suffered severe drug resistance [10,11]. Itraconazole is an improvement of fluconazole in terms of having a broader antifungal spectrum and better toleration. However, its use is hampered by variable oral absorption and low bioavailability. This situation has led to an ongoing search for new azoles and several novel azoles have been developed with improved profiles. The second generation of azoles (Fig. 1), such as voriconazole [12], posaconazole [13], ravuconazole [14] and albaconazole [15], is marketed or currently in the late stages of clinical trials. They are noted for their broad antifungal spectrum, low toxicity and improved pharmacodynamic profiles.

Azole antifungals act by competitive inhibition of the lanosterol 14α-demethylase (CYP51), the enzyme that catalyzes the oxidative removal of the 14α-methyl group of lanosterol to give Δ14,15-desaturated intermediates in ergosterol biosynthesis [16]. In yeast and fungi, CYP51 is the key enzyme in sterol biosynthesis. Selective inhibition of CYP51 would cause depletion of ergosterol and accumulation of lanosterol and other 14-methyl sterols resulting in the growth inhibition of fungal cells [17]. Eukaryotic CYP51s are membrane associated proteins and solving their crystal structures remains a challenge. In our continual interest in rational antifungal drug design, we have constructed three-dimensional (3D) models of CYP51 from *Candida albicans* (CACYP51) and *Aspergillus fumigatus* (AFCYP51) through homology modeling [18,19] on the basis of the crystal coordinates of CYP51 from *Mycobacterium tuberculosis* (MTCYP51) [20]. The overall structures of the models are similar to that of the template structure (MTCYP51), which remains the core structural motif characteristic for cytochrome

* Corresponding author. Tel./fax: +86 21 81871243.
** Corresponding author. Tel./fax: +86 21 81871233.
E-mail addresses: shengcq@hotmail.com (C. Sheng), zhangwnk@hotmail.com (W. Zhang).

0223-5234/$ – see front matter © 2009 Elsevier Masson SAS. All rights reserved.
doi:10.1016/j.ejmech.2009.05.018

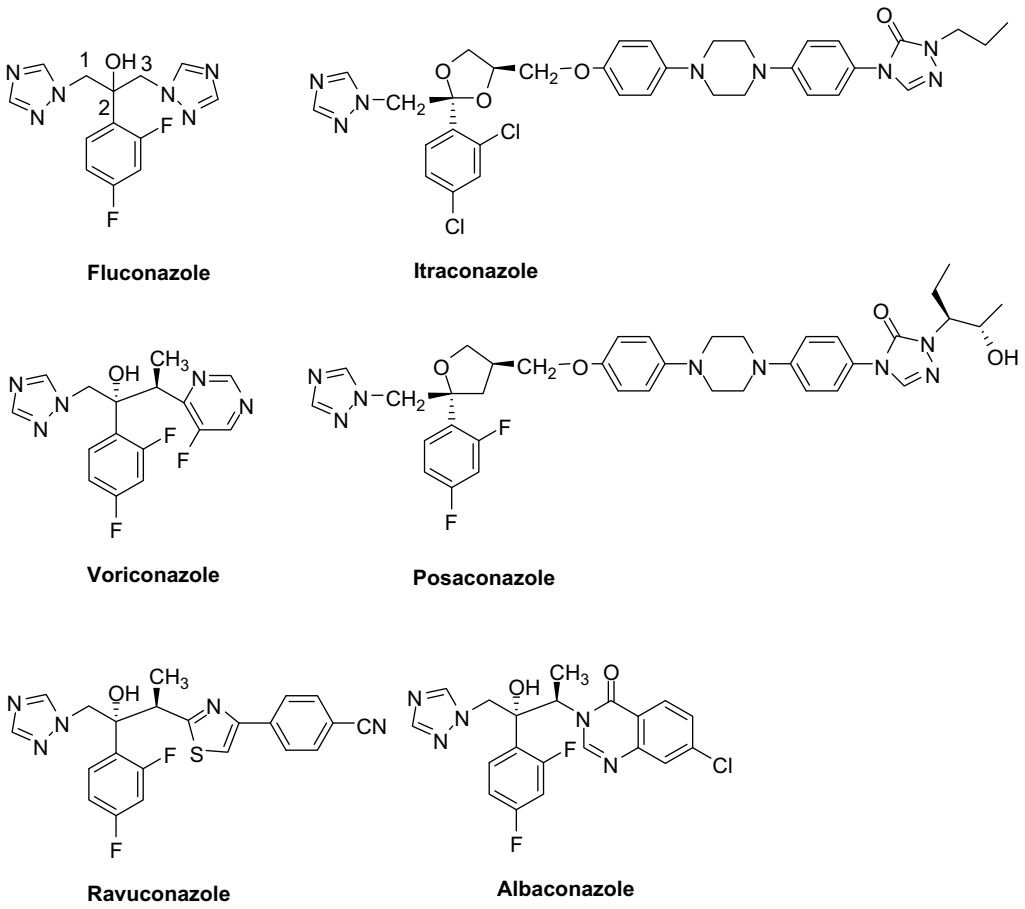

Fig. 1. Chemical structures of azole antifungal agents.

P450 proteins. The structurally and functionally important regions, such as the heme environment, the substrate access channel, and the active site have been recognized accurately. The binding mode of azoles with CACYP51 has been investigated by flexible molecular docking [18,21]. Important residues involved in azole binding are validated by site-directed mutagenesis [22]. The information obtained from molecular modeling greatly facilitates the process of rational antifungal drug design. On the basis of the results from molecular modeling, novel non-azole CACYP51 inhibitors [23] and highly potent new azoles [21] have been discovered successfully, which demonstrates that the utilization of structural information of fungal CYP51s can accelerate the discovery of novel antifungal agents.

In the present study, a series of new azoles with substituted-phenoxypropyl piperazine side chains were designed and synthesized on the basis of the active site of CACYP51. The new azoles reveal excellent *in vitro* antifungal activity with broad spectrum. The structure–activity relationships (SARs) of the azoles were analyzed by molecular docking.

2. Chemistry

As a key intermediate of our designed triazole antifungals, the oxirane compound **4** was synthesized by our reported procedure (Scheme 1) [21]. The phenoxyalkylpiperazine side chains **7a–c** were synthesized via three steps. Excess dibromoalkanes **5a–c** were treated with phenol to give bromoalkyloxybenzenes **6a–c**. Compounds **6a–c** were subsequently reacted with piperazine in the presence of potassium carbonate and DMF at 80 °C to afford side chains **7a–c**. The target compounds **8a–c** were obtained as racemates by treating epoxide **4** with side chains **7a–c** in the presence of triethylamine and ethanol at 80 °C with moderate to high yields. The target compounds **12a–n** (racemates) were obtained by a similar procedure (Scheme 2). The nitro groups on the phenyl ring of **12h**, **12m** and **12n** were reduced to amino groups in the presence of Raney Ni and hydrazine hydrate to give **12o**, **12p** and **12q**, respectively (Scheme 3). Compound **12h** was converted to **12r** and **12s** by reacting with corresponding acyl chloride in the presence of triethylamine and CH_2Cl_2 at room temperature (Scheme 4).

3. Pharmacology

In vitro antifungal activity was measured by means of the MIC using the serial dilution method in 96-well microtest plates. Test fungal strains were obtained from the ATCC or were clinical isolates. The MIC determination was performed according to the National Committee for Clinical Laboratory Standards (NCCLS) recommendations with RPMI 1640 (Sigma) buffered with 0.165MMOPS (Sigma) as the test medium. The MIC value was defined as the lowest concentration of test compounds that resulted in a culture with turbidity less than or equal to 80% inhibition when compared with the growth of the control. Test compounds were dissolved in DMSO serially diluted in growth medium. The yeasts were incubated at 35 °C and the dermatophytes at 28 °C.

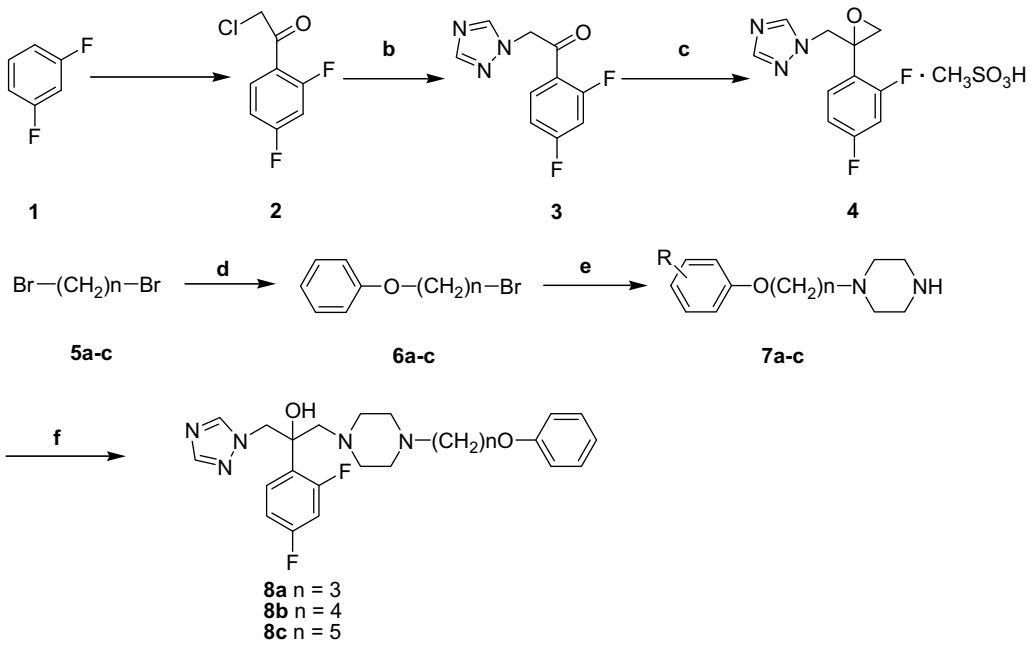

Scheme 1. Reagents and conditions: a. $ClCH_2COCl$, $AlCl_3$, CH_2Cl_2, 40 °C, 3 h, 50%; b. triazole, K_2CO_3, CH_2Cl_2, rt, 24 h, 70.0%; c. $(CH_3)_3SOI$, NaOH, toluene, 60 °C, 3 h, 62.3%; d. phenol, K_2CO_3, DMF, rt, 24 h, 91.8–92.3%; e. piperazine, K_2CO_3, EtOH, 70 °C, 8 h, 90.5–95.2%; f. **4**, Et_3N, EtOH, reflux, 9 h, 29.8–40.1%.

Growth MIC was determined at 24 h for *Candida* species, at 72 h for *Cryptococcus neoformans*, and at 7 days for filamentous fungi.

4. Results and discussion

4.1. Rational design of the new azoles

In our previous studies, azole–CACYP51 interactions have been explored by flexible molecular docking [18,21]. Moreover, the active site of CACYP51 has been characterized by multiple copy simultaneous search (MCSS) [23]. As discussed earlier [23], the active site of CACYP51 can be divided into four pockets. The S1 pocket represents the hydrophilic hydrogen bond binding site. The S2 pocket is above the heme ring representing the core hydrophobic area. The S3 pocket represents the narrow and hydrophobic cleft (facing BC loop). The S4 pocket represents a hydrophobic hydrogen bond binding site (facing FG loop), which is important for the optimization of the C3-side chain of azole antifungal agents. Our docking studies indicate that the triazoyl ring of azole antifungal agents binds to the S2 pocket through the formation of a coordination bond with iron of heme group. The difluorophenyl or dichlorophenyl group is located in the S3 pocket and forms hydrophobic interaction with Ala114, Phe126, Leu139, Ile304 and Met306. In the crystal structure of MTCYP51 in complex with fluconazole [20], the active site is filled with water molecules and fluconazole interacts with at least three water molecules. From our previous docking models [21], the hydroxyl group attached to C2 was supposed to interact with the S1 pocket through the hydrogen-bonding interaction with His310 mediated by crystal waters as found in MTCYP51–fluconazole complex. Different side chains attached to C3 are located in the S4 pocket and form hydrophobic and van der Waals interactions. Because most of the recent efforts on the optimization of azole antifungal agents have been focused on the modification of the side chain attached to C3 [21,24–26], the triazoyl ring, difluorophenyl group and C2 hydroxyl group were retained as essential pharmacophoric elements in the present study. Considering the hydrophobic nature of the C4 pocket of CACYP51, a hydrophobic side chain is necessary, while an additional

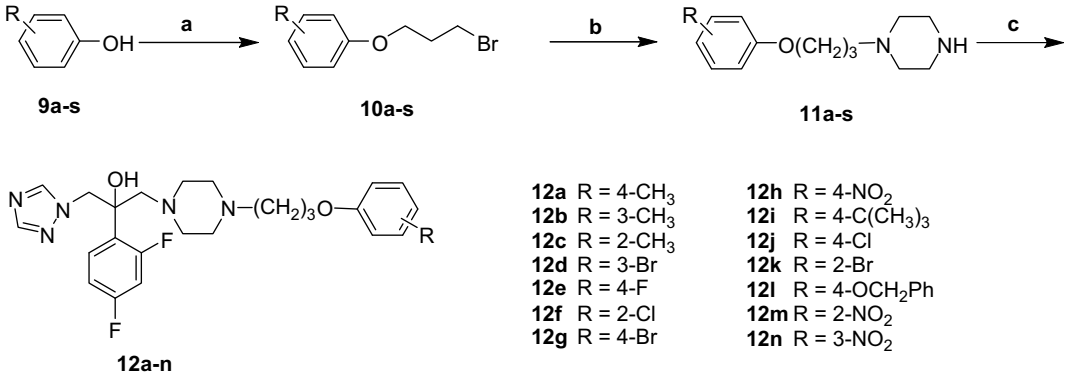

Scheme 2. Reagents and conditions: a. substitute phenol, K_2CO_3, DMF, rt, 24 h, 90.8–94.2%; b. piperazine, K_2CO_3, EtOH, 70 °C, 8 h, 90.1–93.6%; c. **4**, Et_3N, EtOH, reflux, 9 h, 29.8–40.1%.

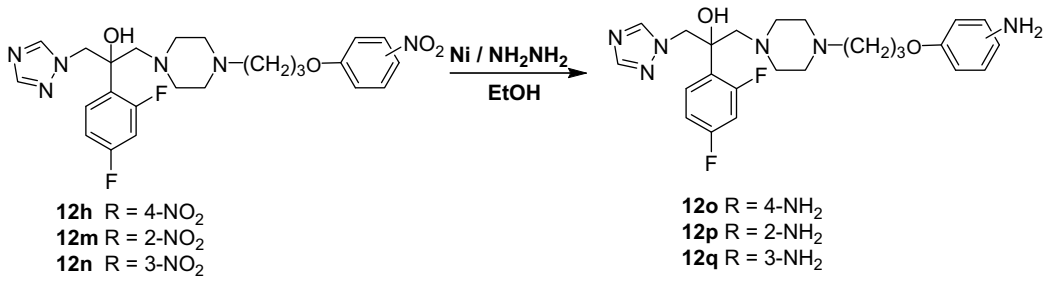

Scheme 3.

hydrogen-bonding interaction will further improve the affinity and specificity of the inhibitors. In the present study, Ser378 was selected as a hydrogen-bonding target, because it was well validated in our previous inhibitor design [21,23]. Moreover, Ser378 is conserved across the fungal CYP51 enzymes, but the corresponding residue in human is Ile379. Therefore, using Ser378 as a hydrogen-bonding target may also improve the selectivity of the inhibitors toward fungal CYP51. On the basis of the above hypothesis, we designed compound **8a** with a phenoxypropyl piperazine side chain. Besides the hydrophobic interactions, the oxygen atom of the side chain was supposed to form a hydrogen bond with Ser378. In order to validate the hypothesis, compound **8a** was docked into the active site of CACYP51. The binding mode of compound **8a** revealed that the phenoxypropyl piperazine side chain was oriented into the S4 pocket with an extended conformation (Fig. 2). The propylpiperazinyl group formed hydrophobic and van der Waals interactions with Leu376, Ile379, Leu461 and Val519. Hydrogen-bonding interaction between the oxygen atom and Ser378 was observed and the terminal phenyl group interacted with surrounding hydrophobic residues such as Phe72 and Met374. Compared to fluconazole, compound **8a** bound to CACYP51 with a lower value of interaction energy (Table 1). In order to test the importance of the propyl group, compounds **8b**–**c** were synthesized. Moreover, compounds **12a**–**s** were designed to investigate the effect of various substitutions attached to the terminal phenyl group on the antifungal activity.

4.2. In vitro antifungal activities

In vitro antifungal activity assay (Table 2) indicates that all the synthesized compounds show moderate to excellent activity against all the tested fungal pathogens. The target compounds revealed the highest activity against *C. albicans* and *Candida parapsilosis*. Most of the compounds are more potent than fluconazole and itraconazole with their minimal inhibitory concentration (MIC_{80}) values in the range of 0.06–0.016 μg/mL. On the *C. neoformans* strain, most of the compounds show higher activity than fluconazole. The MIC_{80} value of compound **12i** against *C. neoformans* is 0.06 μg/mL, indicating that its activity is comparable to that of voriconazole. Fluconazole is not effective against *A. fumigatus*, while our compounds show moderate activity. The MIC_{80} values of compounds **12g**, **12i** and **12l** against *A. fumigatus* are in the range of 1–2 μg/mL. Moreover, the designed compounds also show good activity against dermatophytes (i.e. *Trichophyton rubrum* and *Microsporum gypseum*). For example, compounds **12i** and **12j** are 4–32 fold more potent against *T. rubrum* than fluconazole, itraconazole and voriconazole. In clinic, azole antifungal agents have suffered serious drug resistance [27] and it is of great significance to find new azoles with activity against resistant clinical isolates. Most of the designed compounds show good inhibitory activity against an azole-resistant strain with their MIC_{80} values in the range of 0.25–0.125 μg/mL. Compound **12i** exhibited the highest activity with broad antifungal spectrum, which is a good candidate for further evaluation.

4.3. SARs of the azoles

We first varied the alkyl length attached to the piperazinyl group. When the propyl group (compound **8a**) is replaced by butyl group (compound **8b**) or pentyl group (compound **8c**), the antifungal activity is decreased. From the docking model, the oxygen atom of phenyl group of compound **8a** forms a hydrogen bond with Ser378 of CACYP51. The hydrogen bond will be broken if the propyl group of compound **8a** is extended, which results in the decrease of the antifungal activity. Then, the effect of the substitutions at the phenol group on the antifungal activity was evaluated. The *in vitro* antifungal activity assay indicates that 4-substituted and 3-substituted derivatives show higher antifungal activity compared to 2-substituted derivatives. The docking model shows that the active site of CACYP51 at position 2 of the bound compound is not large enough to accommodate an additional group. However, positions 3 and 4 of the phenol group contain an extra small pocket defined by Met374, Tyr69 and Phe72. Among the 4-substituted derivatives, halogen and alkyl substituted compounds (e.g. compounds **12a**, **12g**, and **12i**) show lower interaction energies with CACYP51 than unsubstituted compound **8a**, because these substitutions formed additional hydrophobic interactions with Met374,

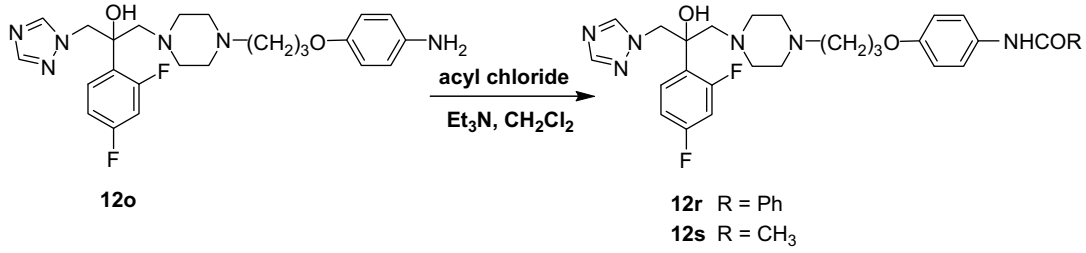

Scheme 4.

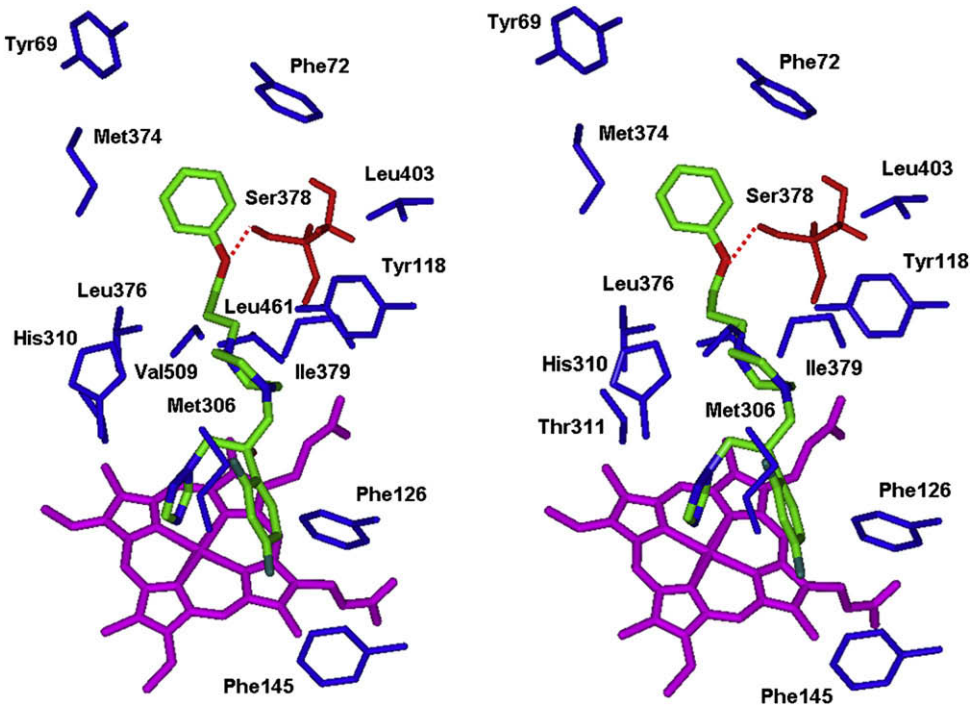

Fig. 2. Stereoview of the docking conformation of compound **8a** (stick model) in the active site of CACYP51. The residues interacting with compound **8a** are shown and hydrogen bonds are displayed through red dotted lines.

Tyr69 and Phe72. Although 4-halogen or 4-alkyl substituted derivatives show the same MIC value against *C. albicans* as compound **8a**, the broader antifungal spectrum of these compounds is observed. Moreover, these compounds show higher activity against *C. albicans* from a fluconazole-resistant isolate than compound **8a**. This result is in good agreement with the previous observation that the additional hydrophobic interaction serves to stabilize the binding of these azoles to the mutated CYP51 proteins, which is important for the reservation of the activity against clinical resistant isolates [28]. If these hydrophobic groups are replaced by a more hydrophilic nitro group (compound **12h**) or amino group (compound **12o**), the antifungal activity is decreased. For the compounds with large substitutions at position 4 (i.e. compounds **12l**, **12r** and **12s**), their antifungal activities are not as good as those of **8a**, possibly because of the steric crowding. The docking model reveals that the terminal phenyl group of **8a** is near the entrance of substrate access channel (FG loop), the side chains of compounds **12l**, **12r** and **12s** are too long to be accommodated in the active site.

5. Conclusion

In summary, computer modeling was used to rational design novel antifungal azoles. On the basis of the active site of CACYP51, a series of new azoles with substituted-phenoxypropyl piperazine side chains were designed and synthesized. Besides the hydrophobic and *van der Waals* interactions with CACYP51, a new hydrogen-bonding interaction with Ser378 was introduced into our designed compounds to improve the affinity and specificity. *In vitro* antifungal activity assay indicates that the new azoles show good activity against important fungal pathogens. Interestingly, the compounds are also active against azole-resistant clinical strain. Several compounds (such as **12i**, **12j** and **12n**) show high *in vitro* antifungal activity with broad spectrum, which were valuable for further evaluation. The structure–activity relationships (SARs) of the compounds were explained by flexible molecular docking. The propyl of the compounds is found important for the maintaining the hydrogen-bonding interaction. A small hydrophobic group is favorable at the position 3 or position 4 of the terminal phenyl group, possibly because of the additional hydrophobic interaction with CACYPY51. Our structure-based inhibitor design for CACYP51 reveals the robustness and efficiency of computer modeling in structural optimization of azole antifungal agents.

Table 1
Calculated interaction energies (kcal/mol) for the complexes of representative compounds with the active site of CACYP51.

Compounds	E_{vdw}	E_{elect}	E_{total}
8a	−77.3	−1.2	−78.5
12a	−81.5	−1.4	−82.9
12g	−78.1	−0.8	−78.9
12h	−70.4	−0.6	−71.0
12i	−87.6	−0.7	−88.3
12o	−71.3	−2.3	−73.6
Fluconazole	−54.8	−3.2	−58.0

6. Experimental protocols

6.1. General procedure for the synthesis of compounds

Nuclear magnetic resonance (NMR) spectra were recorded on a Bruker 500 spectrometer with TMS as an internal standard and $CDCl_3$ as solvent. Chemical shifts (δ values) and coupling constants (J values) are given in ppm and Hz, respectively. ESI mass spectra were performed on an API-3000 LC–MS spectrometer. Elemental analyses were performed with a MOD-1106 instrument and were consistent with theoretical values within ±0.4%. TLC analysis was carried out on silica gel plates GF254 (Qindao Haiyang Chemical, China). Silica gel column chromatography was performed with Silica gel 60G (Qindao Haiyang Chemical, China). Commercial solvents were used without any pretreatment.

Table 2
Antifungal *in vitro* activities of the compounds (MIC_{80}, μg mL^{-1}).[a]

Compounds	*C. albicans*	*C. albicans* (R)[b]	*C. neoformans*	*C. tropicalis*	*T. rubrum*	*A. fumigatus*	*M. gypseum*
8a	0.0156	64	1	0.0625	0.25	32	4
8b	0.25	32	1	0.25	1	8	4
8c	0.0625	4	1	0.0625	0.25	32	4
12a	0.0156	0.12	0.25	0.0625	0.0625	8	0.25
12b	0.0156	0.125	1	0.0625	0.25	16	1
12c	0.0625	0.125	1	0.0625	0.25	32	1
12d	0.0156	16	0.25	0.0156	0.0625	4	0.25
12e	0.0156	32	1	0.0625	0.25	32	1
12f	0.0625	16	1	0.0625	0.25	32	1
12g	0.0156	0.25	0.25	0.0156	0.0625	1	0.25
12h	0.0625	0.125	0.25	0.0625	0.0625	32	1
12i	0.0156	0.125	0.0625	0.0156	0.0156	2	0.0625
12j	0.0156	0.125	0.25	0.0156	0.0156	4	0.25
12k	0.0625	8	1	0.0156	0.25	16	1
12l	0.0625	32	0.25	0.0625	0.0625	2	0.0625
12m	0.25	2	4	0.25	1	64	4
12n	0.0625	0.25	0.25	0.0156	0.0625	32	0.25
12o	0.25	0.25	4	1	4	64	16
12p	0.25	0.5	4	0.25	1	64	16
12q	1	0.25	16	1	4	>64	64
12r	0.25	0.5	16	1	16	>64	64
12s	0.25	2	1	0.25	0.25	>64	4
FLZ	1	>64	1	1	4	>64	16
ITZ	0.125	>64	0.125	0.125	0.125	2	0.25
VOR	0.0625	>64	0.0625	0.0625	0.0625	0.5	0.0625

[a] Abbreviations: *C. albicans*, *Candida albicans*; *C. neoformans*, *Cryptococcus neoformans*; *C. tropicalis*, *Candida tropicalis*; *T. rubrum*, *Trichophyton rubrum*; *A. fumigatus*, *Aspergillus fumigatus*; *M. gypseum*, *Microsporum gypseum*; FLZ, Fluconazole; ITZ, Itraconazole; VOR, Voriconazole.
[b] Clinical isolate resistant to FLZ, ITZ and VOR.

*6.1.1. Chemical synthesis of 1-(3-bromopropoxy)-4-methylbenzene (**10a**)*

A solution of 1,3-dibrompropane (20.19 g, 0.10 mol) in 80 mL DMF was added dropwise to a stirred mixture of p-cresol (5.41 g, 0.05 mol), K_2CO_3 (10.35 g, 0.075 mol) and DMF (20 mL) at room temperature. The mixture was stirred at the same temperature for 24 h, diluted with ether (200 mL) and washed by H_2O (200 mL × 3). The organic layer was separated, dried with Na_2SO_4, and concentrated under reduced pressure. The residue was purified by column chromatography (hexane) to give **10a** as yellow oil: 10.57 g, (92.3%). ^{1}H NMR δ (ppm): 6.80–7.09 (m, 4H, Ar–H), 4.07 (t, 2H, J = 5.8 Hz, OCH_2), 3.60 (t, 2H, J = 6.5 Hz, CH_2Br), 2.30–2.34 (m, 2H, $CH_2\underline{CH_2}CH_2$), 2.28 (s, 3H, CH_3). MS (ESI) m/z: 229 (M). The synthetic methods for the following compounds **6a–c** and **10b–n** were similar to the synthesis of compound **10a**.

*6.1.2. Chemical synthesis of 1-(3-(p-tolyloxy)propyl)piperazine (**11a**)*

A solution of compound **10a** (2.29 g, 0.01 mol) in EtOH (20 mL) was added dropwise to a stirred mixture of piperazine (1.04 g, 0.012 mol), K_2CO_3 (2.08 g, 0.015 mol) and EtOH (10 ml). Then, the mixture was heated to reflux for 8 h. After filtration, the solvent was evaporated under reduced pressure to give **11a** as solid, 1.86 g, (79.49%). The product was used in the next step without further purification. ^{1}H NMR δ (ppm): 6.77–7.08 (m, 4H, Ar–H), 3.97 (t, 2H, J = 6.2 Hz, OCH_2), 2.64–3.12 (m, 8H, piperazine–H), 2.57 (t, 2H, J = 7.1 Hz, piperazine–$C\underline{H_2}$), 2.28 (s, 3H, CH3), 1.92–1.96 (m, 2H, $CH_2\underline{CH_2}CH_2$). MS (ESI) m/z: 235 (M + 1). The synthetic methods for the following compounds **7a–c** and **11b–n** were similar to the synthesis of compound **11a**.

*6.1.3. Chemical synthesis of 2-(2,4-difluorophenyl)-3-(4-(3-(p-tolyloxy)propyl) piperazin-1-yl)-1-(1H-1,2,4-triazol-1-yl)propan-2-ol (**12a**)*

A solution of epoxide **4** (1.00 g, 0.003 mol), **11a** (0.94 g, 0.004 mol), triethylamine (2 mL) and EtOH (20 mL) was heated to reflux for 12 h. The solvent was evaporated under reduced pressure. The residue was purified by silica gel column chromatography (CH_2Cl_2:MeOH 100:2, v/v) to give **12a** as pale yellow oil, 0.54 g (38.2%). ^{1}H NMR δ (ppm): 8.13 (s, 1H, TriazC$_3$–H), 7.78 (s, 1H, TriazC$_5$–H), 6.75–7.55 (m, 7H, Ar–H), 4.51 (dd, 2H, J_1 = 5.2 Hz, J_2 = 14.3 Hz, C$_1$–H), 3.93 (t, 2H, J = 6.3 Hz, OCH_2), 3.07 (d, 1H, J = 13.6 Hz, C$_3$–Ha), 2.66 (d, 1H, J = 13.6 Hz, C$_3$–Hb), 2.45 (t, 2H, J = 7.4 Hz, piperazine–$C\underline{H_2}$), 2.37 (br, 8H, piperazine–H), 2.27 (s, 3H, $PhC\underline{H_3}$), 1.89 (br, 2H, $CH_2\underline{CH_2}CH_2$). ^{13}C NMR δ (ppm): 161.51, 157.74, 156.62, 150.77, 144.45, 129.63, 129.14, 126.04, 114.16, 111.32, 104.06, 71.76, 65.90, 62.10, 56.17, 56.76, 54.12, 52.98, 26.51, 20.24. MS (ESI) m/z: 472 (M + 1). Anal. calcd. for $C_{25}H_{31}F_2N_5O_2$: C, 63.68; H, 6.63; N, 14.85. Found: C, 63.76; H, 6.62; N, 14.82.

The synthetic methods for the target compounds **8a–c** and **12b–n** were similar to the synthesis of compound **12a**.

*6.1.4. Chemical synthesis of 3-(4-(3-(4-aminophenoxy)propyl)piperazin-1-yl)-2-(2,4-difluorophenyl)-1-(1H-1,2,4-triazol-1-yl)propan-2-ol (**12o**)*

Catalytic amount of Raney Ni was added to the solution of **12h** (0.2 g, 0.0004 mol) in 5 mL alcohol in the presence of hydrazine hydrate (1 mL). The mixture was stirred at room temperature for 5 h. The solid was separated, and the filtrate was evaporated under reduced pressure. The residue was purified by column chromatography (CH_2Cl_2:MeOH 100:5, v/v) to give **12o** as brown oil, 0.18 g (92.3%). ^{1}H NMR δ (ppm): 8.13 (s, 1H, TriazC$_3$–H), 7.78 (s, 1H, TriazC$_5$–H), 6.60–7.54 (m, 7H, Ar–H), 4.51 (dd, 2H, J_1 = 3.8 Hz, J_2 = 14.2 Hz, C$_1$–H), 3.88 (t, 2H, J = 6.3 Hz, OCH_2), 3.06 (d, 1H, J = 13.5 Hz, C$_3$–Ha), 2.67 (d, 1H, J = 13.6 Hz, C$_3$–Hb), 2.48 (t, 2H, J = 6.0 Hz piperazine–$C\underline{H_2}$), 2.39 (br, 8H, piperazine–H), 1.87 (br, 2H, $CH_2\underline{CH_2}CH_2$). ^{13}C NMR δ (ppm): 162.64, 159.79, 157.82, 152.64, 150.79, 144.65, 129.22, 126.19, 117.38, 114.70, 111.44, 104.16, 71.68, 66.86, 62.25, 56.30, 54.90, 54.13, 53.03, 26.59. MS (ESI) m/z: 471 (M − 1). Anal. calcd. for $C_{24}H_{30}F_2N_6O_2$: C, 61.00; H, 6.40; N, 17.79. Found: C, 61.06; H, 6.39; N, 17.76.

The synthetic methods for the target compounds **12p** and **12q** were similar to the synthesis of compound **12o**.

*6.1.5. Chemical synthesis of 3-(4-(3-(4-benzamidophenoxy)propyl)piperazin-1-yl)-2-(2,4-difluorophenyl)-1-(1H-1,2,4-triazol-1-yl)propan-2-ol (**12r**)*

A solution of benzoyl chloride (0.007 g, 0.046 mmol) in 5 mL methanol was added dropwise to the solution of **12o** (0.02 g, 0.042 mmol), triethylamine (1 mL), and CH_2Cl_2 (5 mL) at 0 °C. The mixture was stirred at room temperature for 5 h. The solvent was evaporated under reduced pressure. The residue was purified by column chromatography (CH_2Cl_2:MeOH 100:2, v/v) to give **12r** as yellow oil, 0.02 g (90.9%). ^{1}H NMR δ (ppm): 8.31 (s, 1H, TriazC$_3$–H), 7.86 (s, 1H, TriazC$_5$–H), 7.85 (s, 1H, NHCO), 6.80–7.79 (m, 13H, Ar–H), 4.54 (dd, 2H, $J_1 = 3.8$ Hz, $J_2 = 14.3$ Hz, C$_1$–H), 4.00 (t, 2H, $J = 6.1$ Hz, OCH$_2$), 3.09 (d, 1H, $J = 13.5$ Hz, C$_3$–Ha), 2.72 (d, 1H, $J = 13.3$ Hz, C$_3$–Hb), 2.52 (br, 10H, piperazine–H, piperazine–CH$_2$), 2.08 (br, 2H, CH$_2$CH$_2$CH$_2$). MS (ESI) m/z: 577 (M + 1). Anal. calcd. for $C_{31}H_{34}F_2N_6O_3$: C, 64.57; H, 5.94; N, 14.57. Found: C, 64.51; H, 5.96; N, 14.62.

The synthetic method for compound **12s** was similar to the synthesis of compound **12r**.

*6.1.6. 2-(2,4-Difluorophenyl)-3-(4-(3-phenoxypropyl)piperazin-1-yl)-1-(1H-1,2,4-triazol-1-yl)propan-2-ol (**8a**)*

^{1}H NMR δ (ppm): 8.13 (s, 1H, TriazC$_3$–H), 7.78 (s, 1H, TriazC$_5$–H), 6.77–7.55 (m, 8H, Ar–H), 5.30 (br, 1H, OH), 4.52 (dd, 2H, $J_1 = 2.1$ Hz, $J_2 = 14.7$ Hz, C$_1$–H), 3.96 (t, 2H, $J = 6.3$ Hz, OCH$_2$), 3.07 (d, 1H, $J = 13.5$ Hz, C$_3$–Hb), 2.66 (d, 1H, $J = 13.5$ Hz, C$_3$–Ha), 2.47 (t, 2H, $J = 7.8$ Hz, piperazine–CH$_2$), 2.37 (br, 8H, piperazine–H), 1.91 (br, 2H, CH$_2$CH$_2$CH$_2$). MS (ESI) m/z: 458 (M + 1). Anal. calcd. for $C_{26}H_{33}F_2N_5O_2$: C, 63.00; H, 6.39; N, 15.31. Found: C, 62.95; H, 6.41; N, 15.30.

*6.1.7. 2-(2,4-Difluorophenyl)-3-(4-(4-phenoxybutyl)piperazin-1-yl)-1-(1H-1,2,4-triazol-1-yl)propan-2-ol (**8b**)*

^{1}H NMR δ (ppm): 8.15 (s, 1H, TriazC$_3$–H), 7.79 (s, 1H, TriazC$_5$–H), 6.78–7.53 (m, 8H, Ar–H), 5.30 (br, 1H, OH), 4.50 (dd, 2H, $J_1 = 1.5$ Hz, $J_2 = 12.2$ Hz, C$_1$–H), 3.96 (t, 2H, $J = 6.2$ Hz, OCH$_2$), 3.06 (d, 1H, $J = 13.8$ Hz, C$_3$–Ha), 2.62 (d, 1H, $J = 13.5$ Hz, C$_3$–Hb), 2.55 (t, 2H, $J = 7.5$ Hz, piperazine–CH$_2$), 2.36 (br, 8H, piperazine–H), 1.74–7.77 (m, 2H, CH$_2$CH$_2$CH$_2$CH$_2$), 1.62 (br, 2H, CH$_2$CH$_2$CH$_2$CH$_2$). MS (ESI) m/z: 472 (M + 1). Anal. calcd. for $C_{31}H_{34}F_2N_6O_3$: C, 63.68; H, 6.63; N, 14.85. Found: C, 63.62; H, 6.64; N, 14.87.

*6.1.8. 2-(2,4-Difluorophenyl)-3-(4-(5-phenoxypentyl)piperazin-1-yl)-1-(1H-1,2,4-triazol-1-yl)propan-2-ol (**8c**)*

^{1}H NMR δ (ppm): 8.14 (s, 1H, TriazC$_3$–H), 7.78 (s, 1H, TriazC$_5$–H), 6.76–7.58 (m, 8H, Ar–H), 5.29 (br, 1H, OH), 4.47 (dd, 2H, $J_1 = 4.8$ Hz, $J_2 = 10.5$ Hz, C$_1$–H), 3.92 (t, 2H, $J = 6.4$ Hz, OCH$_2$), 3.06 (d, 1H, $J = 13.5$ Hz, C$_3$–Ha), 2.65 (d, 1H, $J = 13.8$ Hz, C$_3$–Hb), 2.36 (br, 8H, piperazine–H), 2.25 (t, 2H, $J = 7.6$ Hz, piperazine–CH$_2$), 1.74–1.78 (m, 2H, CH$_2$CH$_2$CH$_2$CH$_2$CH$_2$), 1.45 (br, 4H, CH$_2$CH$_2$CH$_2$CH$_2$CH$_2$). MS (ESI) m/z: 486 (M + 1). Anal. calcd. for $C_{26}H_{32}F_2N_6O_3$: C, 64.31; H, 6.85; N, 14.42. Found: C, 64.28; H, 6.86; N, 14.42.

*6.1.9. 2-(2,4-Difluorophenyl)-3-(4-(3-(m-tolyloxy)propyl)piperazin-1-yl)-1-(1H-1,2,4-triazol-1-yl)propan-2-ol (**12b**)*

^{1}H NMR δ (ppm): 8.13 (s, 1H, TriazC$_3$–H), 7.78 (s, 1H, TriazC$_5$–H), 6.66–7.55 (m, 7H, Ar–H), 4.51 (dd, 2H, $J_1 = 5.4$ Hz, $J_2 = 14.0$, C$_1$–H), 3.94 (t, 2H, $J = 6.2$ Hz, OCH$_2$), 3.06 (d, 1H, $J = 13.5$ Hz, C$_3$–Ha), 2.66 (d, 1H, $J = 13.5$ Hz, C$_3$–Hb), 2.45 (t, 2H, $J = 7.4$ Hz, piperazine–CH$_2$), 2.37 (br, 8H, piperazine–H), 2.32 (s, 3H, PhCH$_3$), 1.89 (br, 2H, CH$_2$CH$_2$CH$_2$). MS (ESI) m/z: 472 (M + 1). Anal. calcd. for $C_{25}H_{31}F_2N_5O_2$: C, 63.68; H, 6.63; N, 14.85. Found: C, 63.63; H, 6.64; N, 14.88.

*6.1.10. 2-(2,4-Difluorophenyl)-3-(4-(3-(o-tolyloxy)propyl)piperazin-1-yl)-1-(1H-1,2,4-triazol-1-yl)propan-2-ol (**12c**)*

^{1}H NMR δ (ppm): 8.15 (s, 1H, TriazC$_3$–H), 7.80 (s, 1H, TriazC$_5$–H), 6.76–7.53 (m, 7H, Ar–H), 4.53 (dd, 2H, $J_1 = 3.2$ Hz, $J_2 = 14.1$ Hz, C$_1$–H), 3.97 (t, 2H, $J = 6.0$ Hz, OCH$_2$), 3.08 (d, 1H, $J = 13.5$ Hz, C$_3$–Ha), 2.69 (d, 1H, $J = 13.5$ Hz, C$_3$–Hb), 2.46 (t, 2H, $J = 7.3$ Hz, piperazine–CH$_2$), 2.37 (br, 8H, piperazine–H), 2.18 (s, 3H, PhCH$_3$), 2.00 (br, 2H, CH$_2$CH$_2$CH$_2$). MS (ESI) m/z: 472 (M + 1). Anal. calcd. for $C_{25}H_{31}F_2N_5O_2$: C, 63.68; H, 6.63; N, 14.85. Found: C, 63.62; H, 6.64; N, 14.87.

*6.1.11. 3-(4-(3-(3-Bromophenoxy)propyl)piperazin-1-yl)-2-(2,4-difluorophenyl)-1-(1H-1,2,4-triazol-1-yl)propan-2-ol (**12d**)*

^{1}H NMR δ (ppm): 8.13 (s, 1H, TriazC$_3$–H), 7.78 (s, 1H, TriazC$_5$–H), 6.78–7.26 (m, 7H, Ar–H), 5.29 (s, 1H, 2-OH), 4.51 (dd, 2H, $J_1 = 5.6$ Hz, $J_2 = 14.0$ Hz, C$_1$–H), 3.94 (t, 2H, $J = 6.2$ Hz, OCH$_2$), 3.07 (d, 1H, $J = 13.5$ Hz, C$_3$–Ha), 2.67 (d, 1H, $J = 13.5$ Hz, C$_3$–Hb), 2.46 (t, 2H, $J = 7.4$ Hz, piperazine–CH$_2$), 2.39 (br, 8H, piperazine–H), 1.90 (br, 2H, CH$_2$CH$_2$CH$_2$). ^{13}C NMR δ (ppm): 162.43, 159.46, 158.61, 150.63, 144.36, 130.21, 129.05, 125.92, 123.37, 122.45, 117.43, 113.24, 111.22, 103.86, 71.70, 65.98, 62.02, 56.07, 54.44, 52.87, 26.22. MS (ESI) m/z: 537 (M + 1). Anal. calcd. for $C_{24}H_{28}BrF_2N_5O_2$: C, 53.74; H, 5.26; N, 13.06. Found: C, 53.79; H, 5.24; N, 13.04.

*6.1.12. 2-(2,4-Difluorophenyl)-3-(4-(3-(4-fluorophenoxy)propyl)piperazin-1-yl)-1-(1H-1,2,4-triazol-1-yl)propan-2-ol (**12e**)*

^{1}H NMR δ (ppm): 8.14 (s, 1H, TriazC$_3$–H), 7.78 (s, 1H, TriazC$_5$–H), 6.78–7.55 (m, 7H, Ar–H), 4.51 (dd, 2H, $J_1 = 7.3$ Hz, $J_2 = 14.2$ Hz, C$_1$–H), 3.92 (t, 2H, $J = 6.3$ Hz, OCH$_2$), 3.06 (d, 1H, $J = 13.5$ Hz, C$_3$–Ha), 2.66 (d, 1H, $J = 13.6$ Hz, C$_3$–Hb), 2.44 (t, 2H, $J = 7.4$ Hz, piperazine–CH$_2$), 2.35 (br, 8H, piperazine–H), 1.87 (br, 2H, CH$_2$CH$_2$CH$_2$). ^{13}C NMR δ (ppm): 163.67, 161.69, 161.59, 156.13, 150.89, 144.55, 129.22, 126.16, 115.53, 111.44, 104.28, 71.84, 66.60, 52.17, 56.27, 54.76, 54.18, 53.05, 26.53. MS (ESI) m/z: 476 (M + 1). Anal. calcd. for $C_{24}H_{28}F_3N_5O_2$: C, 60.62; H, 5.94; N, 14.73. Found: C, 60.67; H, 5.93; N, 14.69.

*6.1.13. 3-(4-(3-(2-Chlorophenoxy)propyl)piperazin-1-yl)-2-(2,4-difluorophenyl)-1-(1H-1,2,4-triazol-1-yl)propan-2-ol (**12f**)*

^{1}H NMR δ (ppm): 8.14 (s, 1H, TriazC$_3$–H), 7.78 (s, 1H, TriazC$_5$–H), 6.79–7.54 (m, 7H, Ar–H), 4.51 (dd, 2H, $J_1 = 5.3$ Hz, $J_2 = 14.2$ Hz, C$_1$–H), 4.04 (t, 2H, $J = 6.2$ Hz, OCH$_2$), 3.06 (d, 1H, $J = 13.6$ Hz, C$_3$–Ha), 2.66 (d, 1H, $J = 13.6$ Hz, C$_3$–Hb), 2.51 (t, 2H, $J = 7.6$ Hz, piperazine–CH$_2$), 2.37 (br, 8H, piperazine–H), 1.95 (br, 2H, CH$_2$CH$_2$CH$_2$). MS (ESI) m/z: 492 (M + 1). Anal. calcd. for $C_{24}H_{28}ClF_2N_5O_2$: C, 58.59; H, 5.74; N, 14.24. Found: C, 58.64; H, 5.73; N, 14.23.

*6.1.14. 3-(4-(3-(4-Bromophenoxy)propyl)piperazin-1-yl)-2-(2,4-difluorophenyl)-1-(1H-1,2,4-triazol-1-yl)propan-2-ol (**12g**)*

^{1}H NMR δ (ppm): 8.14 (s, 1H, TriazC$_3$–H), 7.78 (s, 1H, TriazC$_5$–H), 6.73–7.56 (m, H, Ar–H), 5.29 (s, 1H, 2-OH), 4.51 (dd, 2H, $J_1 = 6.7$ Hz, $J_2 = 14.2$, C$_1$–H), 3.92 (t, 2H, $J = 6.2$ Hz, OCH$_2$), 3.06 (d, 1H, $J = 13.5$ Hz, C$_3$–Ha), 2.66 (d, 1H, $J = 13.5$ Hz, C$_3$–Hb), 2.43 (t, 2H, $J = 7.1$ Hz, piperazine–CH$_2$), 2.35 (br, 8H, piperazine–H), 1.87 (br, 2H, CH$_2$CH$_2$CH$_2$). ^{13}C NMR δ (ppm): 163.23, 161.29, 157.73, 150.53, 144.29, 131.79, 129.00, 125.91, 115.96, 112.28, 111.20, 103.86, 71.74, 65.95, 62.02, 56.00, 54.40, 53.97, 52.81, 26.19. MS (ESI) m/z: 537 (M + 1). Anal. calcd. for $C_{24}H_{28}BrF_2N_5O_2$: C, 53.74; H, 5.26; N, 13.06. Found: C, 53.69; H, 5.27; N, 13.09.

*6.1.15. 2-(2,4-Difluorophenyl)-3-(4-(3-(4-nitrophenoxy)propyl)piperazin-1-yl)-1-(1H-1,2,4-triazol-1-yl)propan-2-ol (**12h**)*

^{1}H NMR δ (ppm): 8.14 (s, 1H, TriazC$_3$–H), 7.78 (s, 1H, TriazC$_5$–H), 6.78–8.18 (m, 7H, Ar–H), 4.51 (dd, 2H, $J_1 = 9.7$ Hz, $J_2 = 14.2$, C$_1$–H), 4.06 (t, 2H, $J = 6.2$ Hz, OCH$_2$), 3.07 (d, 1H, $J = 13.5$ Hz, C$_3$–Ha), 2.67 (d, 1H, $J = 13.5$ Hz, C$_3$–Hb), 2.46 (t, 2H, $J = 6.4$ Hz, piperazine–CH$_2$), 2.37 (br, 8H, piperazine–H), 1.94 (br, 2H, CH$_2$CH$_2$CH$_2$). MS (ESI) m/z:

501 (M − 1). Anal. calcd. for $C_{24}H_{28}F_2N_6O_4$: C, 57.36; H, 5.62; N, 16.72. Found: C, 57.42; H, 5.61; N, 16.70.

*6.1.16. 3-(4-(3-(4-Tert-butylphenoxy)propyl)piperazin-1-yl)-2-(2,4-difluorophenyl)-1-(1H-1,2,4-triazol-1-yl)propan-2-ol (**12i**)*

^{1}H NMR δ (ppm): 8.14 (s, 1H, TriazC$_3$–H), 7.78 (s, 1H, TriazC$_5$–H), 6.79–7.55 (m, 7H, Ar–H), 4.51 (dd, 2H, J_1 = 5.2 Hz, J_2 = 14.3 Hz, C$_1$–H), 3.94 (t, 2H, J = 6.3 Hz, OCH$_2$), 3.04 (d, 1H, J = 13.5 Hz, C$_3$–Ha), 2.66 (d, 1H, J = 13.5 Hz, C$_3$–Hb), 2.45 (t, 2H, J = 6.7 Hz, piperazine–CH$_2$), 2.36 (br, 8H, piperazine–H), 1.88 (br, 2H, CH$_2$CH$_2$CH$_2$), 1.28 (s, 9H, C(CH$_3$)$_3$). ^{13}C NMR δ (ppm): 166.58, 163.65, 161.66, 157.875, 150.96, 144.58, 129.262, 126.09, 113.87, 111.47, 104.20, 71.81, 65.92, 62.21, 56.32, 54.90, 54.30, 53.13, 33.96, 31.45, 26.70. MS (ESI) *m*/*z*: 514 (M + 1). Anal. calcd. for $C_{28}H_{37}F_2N_5O_2$: C, 65.48; H, 7.26; N, 13.64. Found: C, 65.41; H, 7.27; N, 13.65.

*6.1.17. 3-(4-(3-(4-Chlorophenoxy)propyl)piperazin-1-yl)-2-(2,4-difluorophenyl)-1-(1H-1,2,4-triazol-1-yl)propan-2-ol (**12j**)*

^{1}H NMR δ (ppm): 8.14 (s, 1H, TriazC$_3$–H), 7.78 (s, 1H, TriazC$_5$–H), 6.77–7.55 (m, 7H, Ar–H), 4.51 (dd, 2H, J_1 = 6.5 Hz, J_2 = 14.2 Hz, C$_1$–H), 3.93 (t, 2H, J = 6.3 Hz, OCH$_2$), 3.06 (d, 1H, J = 13.6 Hz, C$_3$–Ha), 2.67 (d, 1H, J = 13.6 Hz, C$_3$–Hb), 2.45 (t, 2H, J = 6.4 Hz, piperazine–CH$_2$), 2.37 (br, 8H, piperazine–H), 1.89 (br, 2H, CH$_2$CH$_2$CH$_2$). ^{13}C NMR δ (ppm): 163.70, 159.74, 157.49, 150.49, 144.58, 129.19, 126.18, 115.69, 111.47, 104.21, 71.86, 66.30, 62.19, 56.30, 54.74, 54.23, 53.10, 26.50. MS (ESI) *m*/*z*: 492 (M + 1). Anal. calcd. for $C_{24}H_{28}ClF_2N_5O_2$: C, 58.59; H, 5.74; N, 14.24. Found: C, 58.62; H, 5.73; N, 14.26.

*6.1.18. 3-(4-(3-(2-Bromophenoxy)propyl)piperazin-1-yl)-2-(2,4-difluorophenyl)-1-(1H-1,2,4-triazol-1-yl)propan-2-ol (**12k**)*

^{1}H NMR δ (ppm): 8.14 (s, 1H, TriazC$_3$–H), 7.78 (s, 1H, TriazC$_5$–H), 6.79–7.55 (m, 7H, Ar–H), 4.51 (dd, 2H, J_1 = 5.4 Hz, J_2 = 14.1 Hz C$_1$–H), 4.03 (t, 2H, J = 6.2 Hz, OCH$_2$), 3.06 (d, 1H, J = 13.6 Hz, C$_3$–Ha), 2.66 (d, 1H, J = 13.6 Hz, C$_3$–Hb), 2.52 (t, 2H, J = 7.2 Hz, piperazine–CH$_2$), 2.36 (br, 8H, piperazine–H), 1.94 (br, 2H, CH$_2$CH$_2$CH$_2$). ^{13}C NMR δ (ppm): 163.62, 161.65, 157.85, 150.92, 144.57, 133.21, 129.25, 128.30, 126.20, 121.69, 113.21, 112.12, 111.45, 104.18, 71.81, 67.08, 62.19, 56.30, 54.70, 53.11, 26.44. MS (ESI) *m*/*z*: 537 (M + 1). Anal. calcd. for $C_{24}H_{28}BrF_2N_5O_2$: C, 53.74; H, 5.26; N, 13.06. Found: C, 53.79; H, 5.24; N, 13.05.

*6.1.19. 3-(4-(3-(4-(Benzyloxy)phenoxy)propyl)piperazin-1-yl)-2-(2,4-difluoro phenyl)-1-(1H-1,2,4-triazol-1-yl)propan-2-ol (**12l**)*

^{1}H NMR δ (ppm): 8.11 (s, 1H, TriazC$_3$–H), 7.78 (s, 1H, TriazC$_5$–H), 6.77–7.42 (m, 12H, Ar–H), 5.00 (s, 2H, PhCH$_2$OPh), 4.52 (dd, 2H, J_1 = 6.2 Hz, J_2 = 14.3 Hz, C$_1$–H), 3.92 (t, 2H, J = 6.1 Hz, OCH$_2$), 3.07 (d, 1H, J = 13.8 Hz, C$_3$–Ha), 2.68 (d, 1H, J = 13.7 Hz, C$_3$–Hb), 2.45 (t, 2H, J = 7.0 Hz, piperazine–CH$_2$), 2.38 (br, 8H, piperazine–H), 1.92 (br, 2H, CH$_2$CH$_2$CH$_2$). MS (ESI) *m*/*z*: 564 (M + 1). Anal. calcd. for $C_{31}H_{35}F_2N_5O_3$: C, 66.06; H, 6.26; N, 12.43. Found: C, 66.00; H, 6.27; N, 12.46.

*6.1.20. 2-(2,4-Difluorophenyl)-3-(4-(3-(2-nitrophenoxy)propyl)piperazin-1-yl)-1-(1H-1,2,4-triazol-1-yl)propan-2-ol (**12m**)*

^{1}H NMR δ (ppm): 8.14 (s, 1H, TriazC$_3$–H), 7.79 (s, 1H, TriazC$_5$–H), 6.80–7.81 (m, 7H, Ar–H), 4.51 (dd, 2H, J_1 = 4.4 Hz, J_2 = 14.2, C$_1$–H), 4.12 (t, 2H, J = 6.1 Hz, OCH$_2$), 3.06 (d, 1H, J = 13.5 Hz, C$_3$–Ha), 2.65 (d, 1H, J = 13.5 Hz, C$_3$–Hb), 2.49 (t, 2H, J = 7.1 Hz, piperazine–CH$_2$), 2.36 (br, 8H, piperazine–H), 1.94 (br, 2H, CH$_2$CH$_2$CH$_2$). ^{13}C NMR δ (ppm): 162.70, 159.61, 152.29, 150.96, 144.64, 139.98, 133.96, 129.33, 126.22, 125.49, 120.19, 114.49, 111.54, 104.24, 71.92, 67.67, 62.27, 56.37, 54.36, 53.13, 26.28. MS (ESI) *m*/*z*: 503 (M + 1). Anal. calcd. for $C_{24}H_{28}F_2N_6O_4$: C, 57.36; H, 5.62; N, 16.72. Found: C, 57.30; H, 5.63; N, 16.74.

*6.1.21. 2-(2,4-Difluorophenyl)-3-(4-(3-(3-nitrophenoxy)propyl)piperazin-1-yl)-1-(1H-1,2,4-triazol-1-yl)propan-2-ol (**12n**)*

^{1}H NMR δ (ppm): 8.13 (s, 1H, TriazC$_3$–H), 7.78 (s, 1H, TriazC$_5$–H), 6.79–7.81 (m, 7H, Ar–H), 5.29 (s, 1H, OH), 4.51 (dd, 2H, J_1 = 6.8 Hz, J_2 = 14.25 Hz, C$_1$–H), 4.05 (t, 2H, J = 6.3 Hz, OCH$_2$), 3.07 (d, 1H, J = 13.6 Hz, C$_3$–Ha), 2.67 (d, 1H, J = 13.6 Hz, C$_3$–Hb), 2.47 (t, 2H, J = 6.1 Hz, piperazine–CH$_2$), 2.38 (br, 8H, piperazine–H), 1.93 (br, 2H, CH$_2$CH$_2$CH$_2$). ^{13}C NMR δ (ppm): 162.45, 161.38, 158.47, 150.67, 148.90, 144.38, 129.61, 129.08, 126.06, 121.30, 115.30, 111.21, 108.50, 103.96, 71.76, 66.50, 62.60, 56.10, 54.30, 54.04, 52.91, 26.12. MS (ESI) *m*/*z*: 503 (M + 1). Anal. calcd. for $C_{24}H_{28}F_2N_6O_4$: C, 57.36; H, 5.62; N, 16.72. Found: C, 57.40; H, 5.61; N, 16.70.

*6.1.22. 3-(4-(3-(3-Aminophenoxy)propyl)piperazin-1-yl)-2-(2,4-difluorophenyl)-1-(1H-1,2,4-triazol-1-yl)propan-2-ol (**12p**)*

^{1}H NMR δ (ppm): 8.12 (s, 1H, TriazC$_3$–H), 7.78 (s, 1H, TriazC$_5$–H), 6.20–7.54 (m, 7H, Ar–H), 4.52 (dd, 2H, J_1 = 3.4 Hz, J_2 = 14.1 Hz, C$_1$–H), 3.92 (t, 2H, J = 6.1 Hz, OCH$_2$), 3.07 (d, 1H, J = 13.4 Hz, C$_3$–Ha), 2.68 (d, 1H, J = 13.4 Hz, C$_3$–Hb), 2.45 (t, 2H, J = 6.2 Hz, piperazine–CH$_2$), 2.37 (br, 8H, piperazine–H), 1.91 (br, 2H, CH$_2$CH$_2$CH$_2$). MS (ESI) *m*/*z*: 471 (M − 1). Anal. calcd. for $C_{24}H_{30}F_2N_6O_2$: C, 61.00; H, 6.40; N, 17.79. Found: C, 60.94; H, 6.42; N, 17.81.

*6.1.23. 3-(4-(3-(2-Aminophenoxy)propyl)piperazin-1-yl)-2-(2,4-difluorophenyl)-1-(1H-1,2,4-triazol-1-yl)propan-2-ol (**12q**)*

^{1}H NMR δ (ppm): 8.12 (s, 1H, TriazC$_3$–H), 7.78 (s, 1H, TriazC$_5$–H), 6.67–7.54 (m, 7H, Ar–H), 4.52 (dd, 2H, J_1 = 3.6 Hz, J_2 = 14.2 Hz, C$_1$–H), 3.99 (t, 2H, J = 6.1 Hz, OCH$_2$), 3.07 (d, 1H, J = 13.4 Hz, C$_3$–Ha), 2.68 (d, 1H, J = 13.4 Hz, C$_3$–Hb), 2.45 (t, 2H, J = 6.4 Hz, piperazine–CH$_2$), 2.38 (br, 8H, piperazine–H), 1.92 (br, 2H, CH$_2$CH$_2$CH$_2$). MS (ESI) *m*/*z*: 471 (M − 1). Anal. calcd. for $C_{24}H_{30}F_2N_6O_2$: C, 61.00; H, 6.40; N, 17.79. Found: C, 60.97; H, 6.41; N, 17.81.

*6.1.24. 2-(2,4-Difluorophenyl)-3-(4-(3-(4-acetamidophenoxy)propyl)piperazin-1-yl)-1-(1H-1,2,4-triazol-1-yl)propan-2-ol (**12s**)*

^{1}H NMR δ (ppm): 8.13 (s, 1H, TriazC$_3$–H), 7.78 (s, 1H, TriazC$_5$–H), 7.02 (s, 1H, NHCOCH$_3$), 6.78–7.54 (m, 7H, Ar–H), 4.52 (dd, 2H, J_1 = 3.8 Hz, J_2 = 14.1 Hz, C$_1$–H), 3.94 (t, 2H, J = 6.1 Hz, OCH$_2$), 3.07 (d, 1H, J = 13.5 Hz, C$_3$–Hb), 2.67 (d, 1H, J = 13.3 Hz, C$_3$–Ha), 2.39 (br, 10H, piperazine–H, piperazine–CH$_2$), 2.15 (s, 3H, CH$_3$), 1.93 (br, 2H, CH$_2$CH$_2$CH$_2$). MS (ESI) *m*/*z*: 515 (M + 1). Anal. calcd. for $C_{26}H_{32}F_2N_6O_3$: C, 60.69; H, 6.27; N, 16.33. Found: C, 60.60; H, 6.28; N, 16.37.

6.2. Flexible docking analysis

The 3D structures of the designed azoles were built by the Builder module within InsightII 2000 software package [29]. Then, the flexible ligand docking procedure in the Affinity module within InsightII was used to define the lowest energy position for the substrate using a Monte Carlo docking protocol. All the atoms within a defined radius (8 Å) of the substrate were allowed to move. The solvation grid supplied with the affinity Program was used. If the resulting substrate/enzyme system was within a predefined energy tolerance of the previous structure, the system was subjected to minimization. The resulting structure was accepted on the basis of energy check, which used the Metropolis criterion, and also a check of RMS distance of the new structure versus the structure found so far. The final conformation was obtained through a simulation annealing procedure from 500 to 300 K, and then 5000 rounds of energy minimization were performed to reach a convergence, where the resulting interaction energy values were used to define a rank order.

Acknowledgement

This work was supported in part by the National Natural Science Foundation of China (Grant No. 30430750) and Shanghai Leading Academic Discipline Project (Project No. B906).

References

[1] S.K. Fridkin, W.R. Jarvis, Clin. Microbiol. Rev. 9 (1996) 499–511.
[2] J.P. Latge, Clin. Microbiol. Rev. 12 (1999) 310–350.
[3] J.N. Steenbergen, A. Casadevall, J. Clin. Microbiol. 38 (2000) 1974–1976.
[4] D.J. Sheehan, C.A. Hitchcock, C.M. Sibley, Clin. Microbiol. Rev. 12 (1999) 40–79.
[5] H.A. Gallis, R.H. Drew, W.W. Pickard, Rev. Infect. Dis. 12 (1990) 308–329.
[6] S. Arikan, J.H. Rex, Curr. Opin. Invest. Drugs 2 (2001) 488–495.
[7] D.W. Denning, J. Antimicrob. Chemother. 49 (2002) 889–891.
[8] J.E. Birnbaum, J. Am. Acad. Dermatol. 23 (1990) 782–785.
[9] R. Cha, J.D. Sobel, Expert Rev. Anti Infect. Ther. 2 (2004) 357–366.
[10] I.A. Casalinuovo, P. Di Francesco, E. Garaci, Eur. Rev. Med. Pharmacol. Sci. 8 (2004) 69–77.
[11] H.L. Hoffman, E.J. Ernst, M.E. Klepser, Expert Opin. Invest. Drugs 9 (2000) 593–605.
[12] P.H. Chandrasekar, E. Manavathu, Drugs Today (Barc) 37 (2001) 135–148.
[13] R. Herbrecht, Int. J. Clin. Pract. 58 (2004) 612–624.
[14] S. Arikan, J.H. Rex, Curr. Opin. Invest. Drugs 3 (2002) 555–561.
[15] J. Capilla, C. Yustes, E. Mayayo, B. Fernandez, M. Ortoneda, F.J. Pastor, J. Guarro, Antimicrob. Agents Chemother. 47 (2003) 1948–1951.
[16] Y. Aoyama, Y. Yoshida, R. Sato, J. Biol. Chem. 259 (1984) 1661–1666.
[17] D.C. Lamb, D.E. Kelly, K. Venkateswarlu, N.J. Manning, H.F. Bligh, W.H. Schunck, S.L. Kelly, Biochemistry 38 (1999) 8733–8738.
[18] H. Ji, W. Zhang, Y. Zhou, M. Zhang, J. Zhu, Y. Song, J. Lu, J. Med. Chem. 43 (2000) 2493–2505.
[19] C. Sheng, W. Zhang, M. Zhang, Y. Song, H. Ji, J. Zhu, J. Yao, J. Yu, S. Yang, Y. Zhou, J. Lu, J. Biomol. Struct. Dyn. 22 (2004) 91–99.
[20] L.M. Podust, T.L. Poulos, M.R. Waterman, Proc. Natl. Acad. Sci. U.S.A. 98 (2001) 3068–3073.
[21] C. Sheng, W. Zhang, H. Ji, M. Zhang, Y. Song, H. Xu, J. Zhu, Z. Miao, Q. Jiang, J. Yao, Y. Zhou, J. Lu, J. Med. Chem. 49 (2006) 2512–2525.
[22] S.H. Chen, C.Q. Sheng, X.H. Xu, Y.Y. Jiang, W.N. Zhang, C. He, Biol. Pharm. Bull. 30 (2007) 1246–1253.
[23] H. Ji, W. Zhang, M. Zhang, M. Kudo, Y. Aoyama, Y. Yoshida, C. Sheng, Y. Song, S. Yang, Y. Zhou, J. Lu, J. Zhu, J. Med. Chem. 46 (2003) 474–485.
[24] N.G. Aher, V.S. Pore, N.N. Mishra, A. Kumar, P.K. Shukla, A. Sharma, M.K. Bhat, Bioorg. Med. Chem. Lett. 19 (2009) 759–763.
[25] F. Giraud, R. Guillon, C. Loge, F. Pagniez, C. Picot, M. Le Borgne, P. Le Pape, Bioorg. Med. Chem. Lett. 19 (2009) 301–304.
[26] N. Lebouvier, F. Pagniez, M. Duflos, P. Le Pape, Y.M. Na, G. Le Baut, M. Le Borgne, Bioorg. Med. Chem. Lett. 17 (2007) 3686–3689.
[27] Z.A. Kanafani, J.R. Perfect, Clin. Infect. Dis. 46 (2008) 120–128.
[28] L. Xiao, V. Madison, A.S. Chau, D. Loebenberg, R.E. Palermo, P.M. McNicholas, Antimicrob. Agents Chemother. 48 (2004) 568–574.
[29] InsightII 2000, Molecular Simulation Inc., 9685 Scranton Road, San Diego, CA 92121-3752, 1999.